Black Hole Masses in X-shaped radio sources

M. Mezcua[1], A.P.Lobanov[1], V.H.Chavushyan[2], J.León-Tavares[2]

[1]Max Planck Institute for Radioastronomy, Bonn, Germany

[2]Instituto Nacional de Astrofísica, Óptica y Electrónica, Puebla, México

Max-Planck-Institut für Radioastronomie

MAX-PLANCK-GESELLSCHAFT

Introduction

X-shaped radio galaxies are a class of extragalactic radio sources with two low-surface-brightness radio lobes (the "wings") oriented at an angle to the active, or high-surface-brightness, lobes. Both sets of lobes pass symmetrically through the center of the elliptical galaxy that is the source of the lobes, giving the galaxy an X-shaped morphology as seen on radio maps.

It has been suggested that the X-shaped morphology can reflect either a recent merger of two Supermassive Black Holes (SMBHs) or the presence of a second active black hole in the galactic nucleus.

This scenario is studied by determining the mass and luminosity of a sample of 22 X-shaped radio galaxies drawn from a list of 100 X-shaped radio source candidates presented by Cheung 2007 using the FIRST (Faint Images of the Radio Sky at Twenty cm) survey. The results are compared to the ones obtained for a sample of 25 radio-loud active nuclei from Marchesini et al. 2004 with similar redshifts ($z < 0.3$) and luminosities whose spectra are found in the SDSS (Sloan Digital Sky Survey).

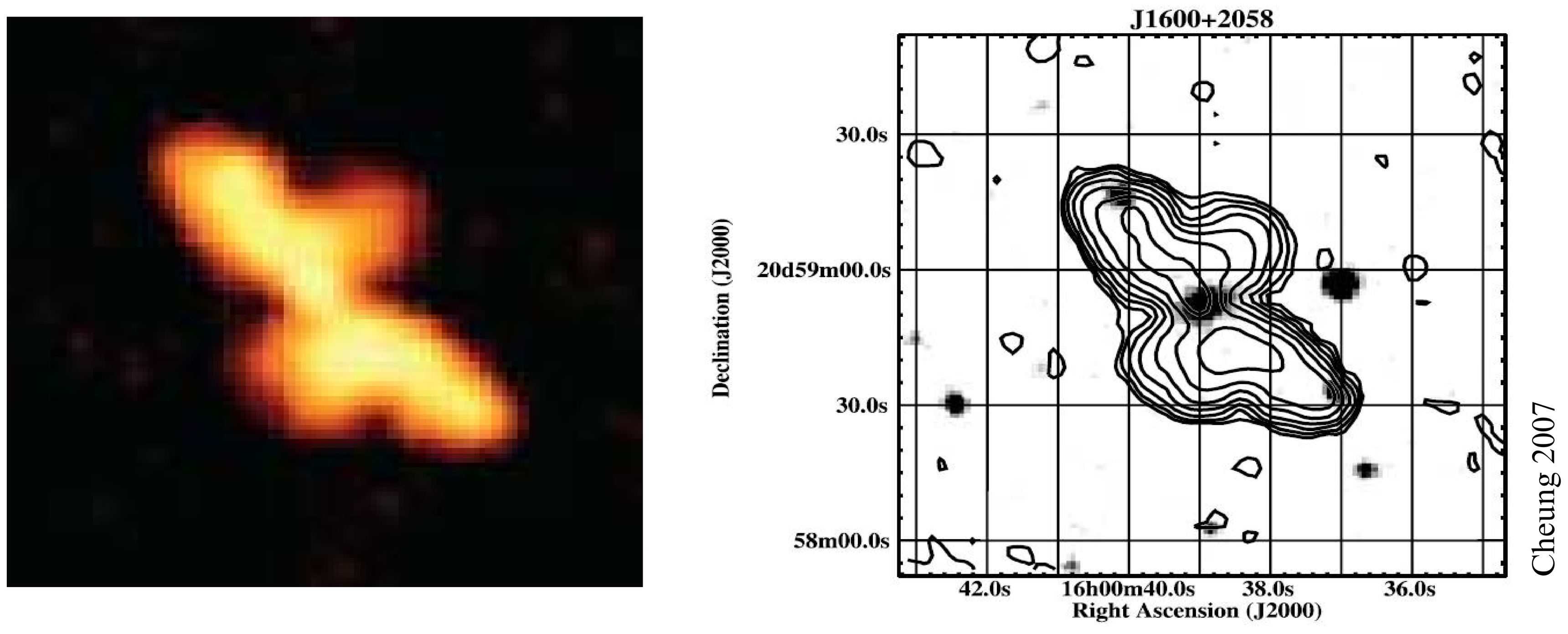

Fig. 1. Images of one of the 100 FIRST X-shaped radio source candidates (J1600+2058). Left, color image from VLA FIRST 1.4GHz. Right, FIRST contours overlaid on the optical image.

Analysis

Our analysis is based on two approaches:

1. Comparing black hole masses in the X-shaped sources and in a sample of radio-loud AGNs with similar radio and optical luminosities and similar optical colors.

2. Comparing black hole masses obtained from stellar velocity dispersion (σ_*) with the ones obtained from the FWHM of the broad emission lines assuming that the gas in the Broad Line Region is virialized (Kaspi et al. 2000). Since a non-active nucleus would contribute to the mass determined from (σ_*) while the virial mass is due only to an active nucleus, this comparison would help us to determine whether X-shaped radio galaxies are formed by an active and a non-active nucleus both remains of the coalescence of two SMBHs.

The 22 X-shaped radio sources analyzed are the only ones from the 100 candidates list from Cheung 2007 that are spectroscopically identified in the latest SDSS data release (DR6).
We used the stellar population synthesis code STARLIGHT (Cid Fernandes et al. 2004) to model the observed spectra of the X-shaped and comparison sample sources. STARLIGHT models each spectrum by a linear combination of synthetic stellar populations and provides the stellar velocity dispersion and the powerlaw continuum flux at 5100Å of the host galaxy.

The modeled spectrum is then subtracted from the observed one as shown in **Fig. 2** and the residual spectrum obtained is used to measure the emission-line parameters.

Assuming that the kinematics of the stars in the bulge of the host galaxies of AGNs reflects the gravitational influence of the central SMBH, the black hole mass M_{BH} can be derived using the relation from Tremaine et al. 2002:

$$M_{BH} = 1.349 \ x \ 10^8 \ M_\odot \ (\frac{\sigma_*}{200 \ km \ s^{-1}})^{4.02 \pm 0.32}$$

Since most of the X-shaped radio galaxies and some of the comparison sample sources are obscured AGNs, their continuum flux cannot be provided by STARLIGHT but using the formula from Wu & Liu 2004:

$$f_{5100Å}(Jy) = 3631 \ x \ 10^{-0.4g} \ [\frac{4700}{5100(1+z)}]^{-(g-r)/2.5log(6231/4770)}$$

where z is the redshift and g and r magnitudes are obtained from SDSS.

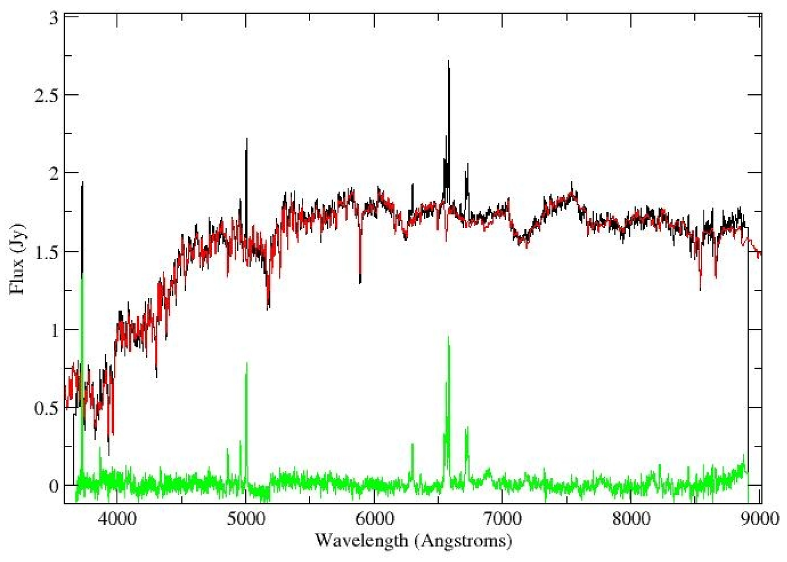

Fig. 2. Spectrum of the X-shaped source J1424+2637.

Table 1

X-shaped

Name	σ_*	log M_{BH} σ_*	log $\lambda L_{5100Å}$ σ_*	log $\lambda L_{5100Å}$ SDSS	log $\lambda L_{1.4GHz}$
	(km/s)	($M_\odot$)	(erg/s)	(erg/s)	(erg/s)
(1)	(2)	(3)	(4)	(5)	(6)
J1424+2637	174.99 ± 6.53	7.90 ± 0.07	40.48 ± 6.37	43.97	39.03
J1207+3352	181.28 ± 3.79	7.96 ± 0.04	41.85 ± 0.84	44.13	38.32
J1043+3131	195.27 ± 8.24	8.09 ± 0.07	41.15 ± 1.15	43.63	38.86
J1140+1057	196.37 ± 7.80	8.10 ± 0.07	40.51 ± 20.11	43.61	38.44
J1040+5056	211.57 ± 15.88	8.23 ± 0.13	-	43.77	37.11
J1330-0206	219.35 ± 7.72	8.29 ± 0.06	-	44.04	36.83
J1210+1121	223.51 ± 9.41	8.32 ± 0.07	-	43.96	36.66
J1455+3237	224.17 ± 5.52	8.33 ± 0.04	41.57 ± 1.78	43.84	36.34
J0924+4233	231.16 ± 15.72	8.38 ± 0.12	-	43.58	37.69
J1444+4147	226.06 ± 9.35	8.34 ± 0.07	-	43.74	37.99
J1327-0203	237.30 ± 9.27	8.43 ± 0.07	-	44.01	39.49
J0838+3253	241.60 ± 11.43	8.46 ± 0.08	-	43.92	36.52
J0813+4347	251.25 ± 5.79	8.53 ± 0.04	-	44.11	37.82
J1111+4050	254.75 ± 4.96	8.55 ± 0.03	-	44.17	38.99
J1005+1154	272.88 ± 6.46	8.67 ± 0.04	-	44.12	37.22
J0049+0059	282.23 ± 9.64	8.73 ± 0.06	-	43.43	36.86
J0001-0033	277.32 ± 4.55	8.70 ± 0.03	-	43.77	35.84
J1339-0016	323.77 ± 4.55	8.97 ± 0.02	-	44.15	37.20
J1625+2705	204.27 ±4.54	8.12 ± 0.04	-	45.13	38.51
J1015+5944	248.16 ± 3.90	8.75 ± 0.02	-	45.18	37.42

Table 2

Marchesini sample

Name	σ_*	log M_{BH} σ_*	log $\lambda L_{5100Å}$ σ_*	log $\lambda L_{5100Å}$ SDSS	log $\lambda L_{1.4GHz}$
	(km/s)	($M_\odot$)	(erg/s)	(erg/s)	(erg/s)
(1)	(2)	(3)	(4)	(5)	(6)
3C197.1	144.35 ± 9.53	7.56 ± 0.12	43.46 ± 0.05	43.80	38.07
3C285	162.58 ± 9.46	7.77 ± 0.10	-	43.86	37.70
3C198	164.35 ± 5.76	7.79 ± 0.06	43.46 ± 0.02	43.66	37.65
3C223	181.42 ± 8.26	7.96 ± 0.08	43.45 ± 0.06	43.81	38.49
3C303	167.41 ± 9.77	7.82 ± 0.10	44.22 ± 0.01	43.96	38.34
3C219	188.98 ± 8.49	8.03 ± 0.08	43.52 ± 0.07	43.96	39.09
3C192	209.94 ± 7.97	8.21 ± 0.07	-	43.85	37.84
1613+27	221.13 ± 6.13	8.31 ± 0.05	42.11 ± 0.40	43.99	36.37
3C227	152.62^a ± 0.39	7.66 ± 0.00	44.63 ± 0.00	43.95	37.49
0755+37	251.55 ± 4.63	8.53 ± 0.03	42.58 ± 0.09	44.48	37.22
3C236	247.41 ± 7.26	8.50 ± 0.05	-	44.17	38.09
3C270	269.46 ± 3.72	8.65 ± 0.02	-	44.04	36.65
3C287.1	246.02 ± 7.86	8.49 ± 0.06	44.24 ± 0.04	44.01	36.29
1527+30	322.89 ± 7.49	8.97 ± 0.01	-	44.29	36.14
3C332	172.37 ± 2.06	7.87 ± 0.02	45.06 ± 4.45	44.05	38.43
1217+023	174.94 ± 1.72	7.84±0.02	-	45.25	38.66
2247+140	229.74 ± 1.56	8.16 ± 0.01	-	44.76	40.25
2349-014	201.97 ± 2.12	8.72 ± 0.01	-	44.95	39.88
1004+130	167.82 ± 1.05	7.77 ± 0.01	-	45.46	39.45
3C277.1	235.9 ± 0.57	8.37 ± 0.00	-	44.62	40.40
3C254	234.2 ± 3.29	8.35 ± 0.03	-	45.81	41.01

Col.(1) Names used in Cheung 2007 and Marchesini et al. 2004 papers. **Col.(2)** Stellar velocity dispersion obtained from STARLIGHT. **Col.(3)** BH mass obtained from the relation of Tremaine et al. 2002. **Col.(4)** Continuum luminosities at 5100Å obtained from the velocity dispersion. **Col.(5)**.Continuum luminosity obtained from SDSS magnitudes. **Col.(6)** Radio luminosity fluxes in 1.4 GHz.

Results

The measure of the width of broad emission lines needed to determine the virial mass was possible in only three X-shaped sources and eleven sources from the comparison sample and therefore it does not allow us to compare these masses with the ones obtained from the velocity dispersion.

To compare the X-shaped radio galaxies sample with the Marchesini sample we plot the continuum luminosity from SDSS magnitudes vs. the radio luminosity at 1.4 GHz and determine a common range of log $\lambda L_{5100Å} \in [43.61, 44.17]$ and log $\lambda L_{1.4GHz} \in [36.29, 39.09]$ (**Fig. 3**). In this common range, the mean M_{BH} is (**Fig. 4**):

- X-shaped sample:

$$M_{BH} = 23.28^{+3.7}_{-3.2} \ x \ 10^7 M_\odot$$

- Comparison sample:

$$M_{BH} = 11.16^{+2.0}_{-1.7} \ x \ 10^7 M_\odot$$

which leads to a mass ratio $r = \frac{mean M_{BH} X\text{-}shaped}{mean M_{BH} Marchesini}$ of $r = 2.09^{+0.4}_{-0.3}$

Since both samples present the same reddening in the u-g vs. g-r diagram (**Fig. 5**), the differences in the mass-luminosity ratios observed in **Fig. 4** are not due to obscuration.
According to Strateva et al. 2001, all the points on top of the u-r = 2.22 separator in the color-color diagram of **Fig. 4** are elliptical galaxies, which correspond to all of the X-shaped sources analyzed.

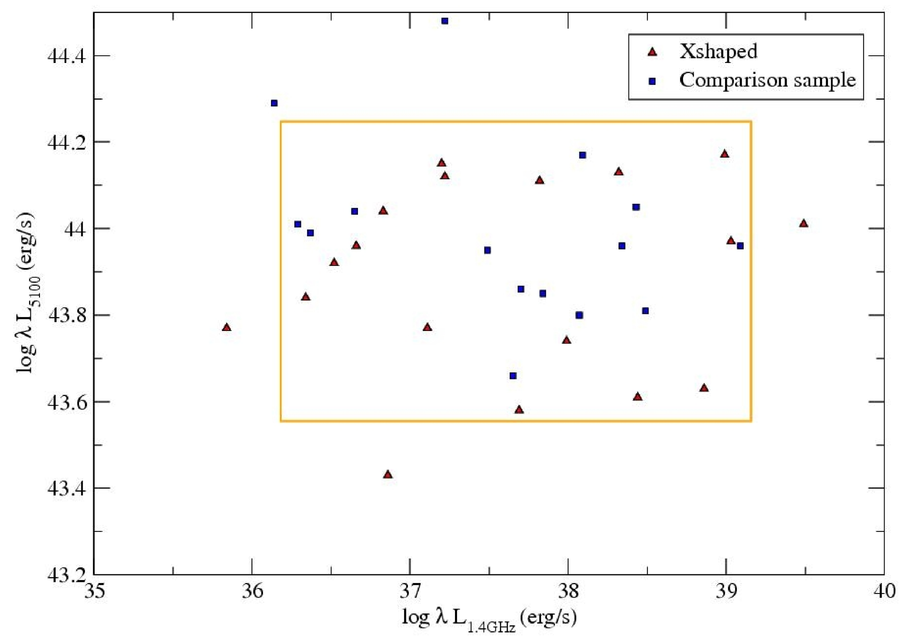

Fig. 3. Continuum luminosity from SDSS vs. radio luminosity. The orange square shows the common range.

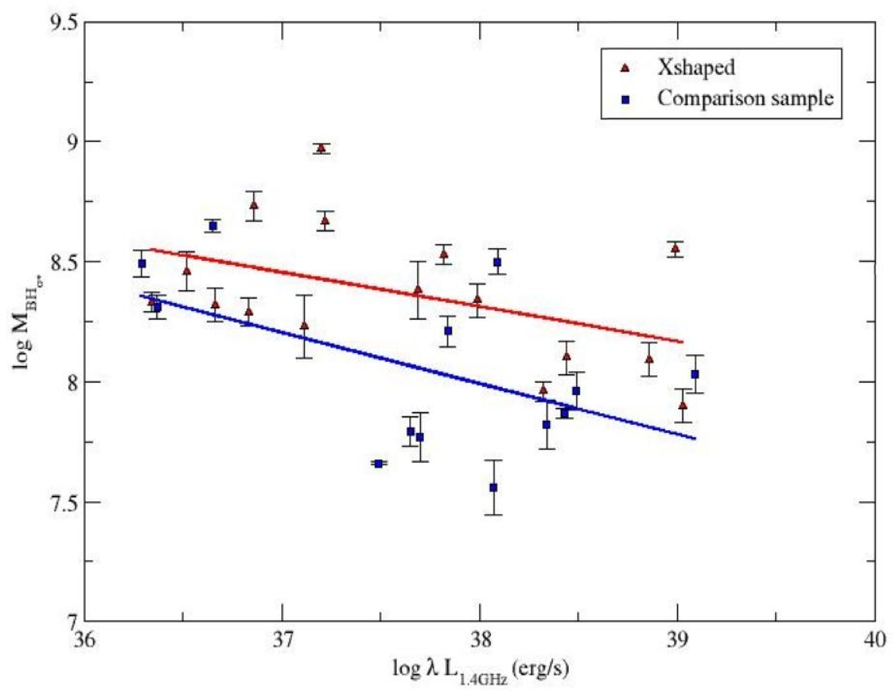

Fig. 4. M_{BH} from the velocity dispersion vs. radio luminosity.

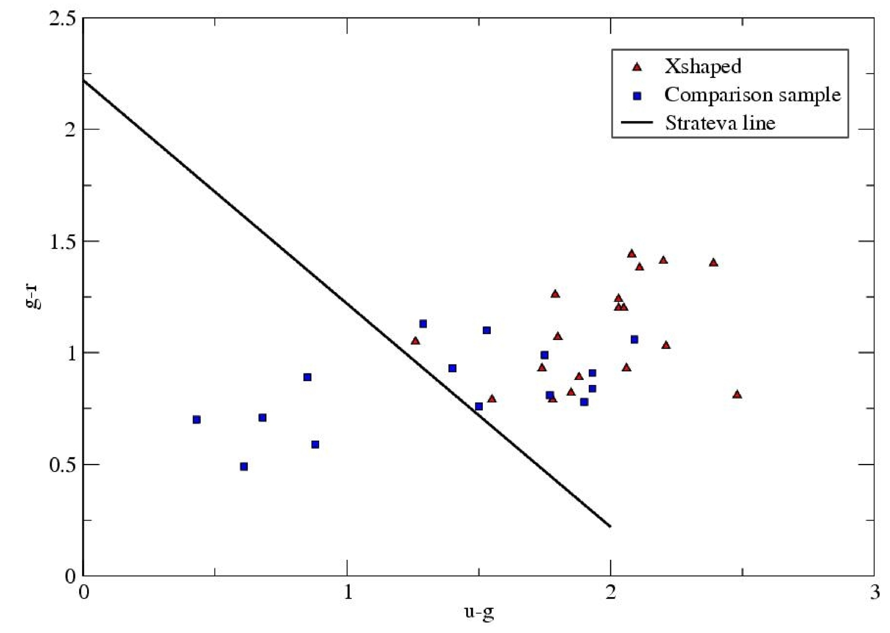

Fig. 5. g-r vs. u-g magnitudes. Black line, u-r =2.22 separator.

Conclusions

Under the merger hypothesis, elliptical galaxies are the product of mergers. Since all the X-shaped sources studied here are shown to be elliptical and are different to the comparison sample at an statistical significance of 1.35σ, the M_{BH} of the X-shaped sample being twice the one of the control sample suggests the possible presence of two central engines in the center of X-shaped radio sources and strengthens the scenario of X-shaped radio sources containing two SMBHs or resulting from a recent coalescence of two SMBHs.

References

Bian, W., Gu, Q., Zhao, Y., Chao, L., & Cui, Q. 2006, MNRAS, 372, 876
Cheung, C.C. 2007, AJ, 133, 2097
Cid Fernandes et al. 2004, MNRAS, 355, 273
Kaspi, S., Smith, P.S., Netzer, H., Maoz, D., Jannuzi, B.T., & Giveon, U. 2000, ApJ, 533, 631
Marchesini, D., Celotti, A., & Ferrarese, L. 2004, MNRAS, 351, 733
Strateva, I., et al. 2001, AJ, 122, 1861
Tremaine, S., et al. 2002, ApJ, 574, 740
Wu, X.-B., & Liu, F.K. 2004, ApJ, 614, 91